Inhibition of Prostate-Specific Antigen (PSA) by α_1-Antichymotrypsin: Salt-Dependent Activation Mediated by a Conformational Change

Ming-Ching Hsieh[‡] and Barry S. Cooperman*[,‡]

Department of Chemistry, University of Pennsylvania, Philadelphia, Pennsylvania 19104-6323

Received August 31, 2001; Revised Manuscript Received November 28, 2001

ABSTRACT: Prostate-specific antigen (PSA) and its SDS-stable complex with the serine proteinase inhibitor (serpin) α_1-antichymotrypsin (ACT), which is the dominant form of PSA in serum, are in widespread use as markers for the diagnosis of prostate cancer, and there is increasing evidence for the involvement of PSA proteinase activity itself in the development of prostate and other cancers. However, both the formation and degradation of the PSA-ACT complex, denoted PSA*ACT* to indicate substantial changes in the structure of both proteins on complex formation, have been incompletely studied. Here we determine rate and equilibrium constants for the steps involved in PSA*ACT* formation and demonstrate that (a) the effects of added NaCl, polyamines, and Zn^{2+} on this process parallel their effects on PSA catalytic activity [Hsieh, M.-C., and Cooperman, B. S. (2000) *Biochim. Biophys. Acta* 1481, 75−87], (b) the effect of added NaCl in dramatically increasing the rate of ACT inhibition of PSA correlates with salt-induced changes in PSA conformation, and (c) the PSA*ACT* complex is subject to proteolysis by human neutrophil elastase. Possible clinical implications of these findings are considered.

The human serine proteinase, prostate-specific antigen (PSA),[1] is a member of the kallikrein family, has chymotrypsin (Chtr)-like specificity, and is found mainly in prostatic tissue and seminal fluid, in which its activity is principally directed toward proteins found in the coagulum secreted by seminal vesicles. It is a glycoprotein of about 28 kDa composed of a single chain polypeptide with one attached carbohydrate chain (*1*). PSA and its SDS-stable complex with the serine proteinase inhibitor (serpin) α_1-antichymotrypsin (ACT), which is the dominant form of PSA in serum, are in widespread use as markers for the diagnosis of prostate cancer (*2*, *3*). There is also increasing evidence for the involvement of PSA activity itself in the development of prostate and other cancers (*4*).

We recently demonstrated an overall similarity in the properties of cloned and refolded recombinant PSA (rPSA) to PSA purified from seminal fluid with respect to its hydrolysis of both a model substrate, S-2586 (3-carbomethoxypropionyl-L-arginyl-L-prolyl-L-tyrosine-*p*-nitroanilide) and several protein substrates (*5*). We also found that added salts, in particular NaCl, give rise to dramatic increases in rPSA catalytic activity, and that Zn^{2+}, spermine, and spermidine, each a major component of seminal and prostatic fluid, strongly inhibit rPSA activity, with Zn^{2+} being a noncompetitive inhibitor while spermine is a competitive inhibitor.

Despite its importance in the diagnosis of prostate cancer, both the formation and degradation of the PSA-ACT complex have been only incompletely studied (*6*, *7*). We denote this complex PSA*ACT* by analogy with the corresponding SDS-stable complex, Chtr*ACT*, that Chtr forms with ACT. Here the asterisks indicate substantial changes in the structure of both ACT and Chtr on complex formation (*8*). PSA*ACT* formation results in cleavage of the Leu358−Ser359 linkage in ACT (*6*). Such cleavage is typical of ACT complexes with serine proteinases, in which the active site Ser is acylated with the 1−358 fragment of ACT (*9*, *10*) and the reaction center loop inserts as an additional strand in β-sheet A.

In this study, we examine the interaction of rPSA with ACT, determining rate and equilibrium constants for the steps involved in PSA*ACT* formation and demonstrating that the effects of added NaCl, polyamines, and Zn^{2+} on this process parallel their effects on PSA catalytic activity. We further demonstrate that the effect of added NaCl in dramatically increasing the rate of ACT inhibition of PSA correlates with salt-induced changes in PSA conformation and that the PSA*ACT* complex is subject to proteolysis by human neutrophil elastase (HNE). These results are potentially important both for the use of PSA as a marker and for efforts to manipulate PSA levels in vivo.

EXPERIMENTAL PROCEDURES

Standard buffer (SB): 50 mM Tris-HCl, pH 7.8 (measured at room temperature).

Materials. S-2586 was purchased from Pharmacia-Hepar-Chromogenix (Franklin, OH). rACT and rPSA were purified as described (*5*, *11*). rACT concentration was determined by titration against standardized Chtr (*11*). The values obtained were typically ∼65% of that estimated by Bradford (*12*) analysis, using a bovine serum albumin standard. All

* To whom correspondence should be addressed. Phone: (215) 898-6330. Fax: (215) 898-2037. E-mail: cooprman@pobox.upenn.edu.

‡ University of Pennsylvania.

[1] Abbreviations: ACT, α_1-antichymotrypsin; Chtr, α-chymotrypsin; DTT, dithiothreitol; HNE, human neutrophil elastase; PAGE, polyacrylamide gel electrophoresis; PSA, prostate specific antigen; S-2586, 3-carbomethoxypropionyl-L-arginyl-L-prolyl-L-tyrosine-*p*-nitroanilide; SB, standard buffer, 50 mM Tris-HCl, pH 7.8; serpin, serine proteinase inhibitor; SI, stoichiometry of inhibition; TCA, trichloroacetic acid.

10.1021/bi0117450 CCC: $22.00
Published on Web 02/08/2002

rPSA concentrations are given as active rPSA, which was determined by titration with standardized rACT at 2.0 M NaCl. The ACT concentration required for full PSA reaction, evaluated using SDS−PAGE analysis and quantitative gel scanning (*13*), was divided by the SI value (the stoichiometry of ACT required for inhibition of 1 equiv of PSA—see Results) to yield the active PSA concentration. The fraction of active rPSA, 78 ± 8% (6 independent determinations), was estimated from the intensity of the band corresponding to rPSA that was unreactive with ACT. Active rPSA concentration was typically 40−45% of that estimated by Bradford analysis.

DTT, iodoacetamide, subtilisins, trichloroacetic acid (TCA), trypsin, and type XVII-B protease were purchased from Sigma (St. Louis, MO). Proteinase K was from Boehringer Mannheim Biochemicals. All salts were obtained from Sigma, ICN Biochemicals, or Fisher Scientific. Midrange protein molecular weight markers were purchased from Promega (Madison, WI). HNE was purchased from CalBiochem (La Jolla, CA). Solvents were from Aldrich, Burdick & Jackson, or Fisher.

Methods. SDS−PAGE Analysis. Proteins were precipitated by addition of an equal amount of 20% TCA, incubated at room temperature for 30 min and isolated by centrifugation at 16000*g* for 10 min. The resultant pellet was dissolved in 10 μL of distilled water, 4 μL of 5× sample buffer (62.6 mM Tris-HCl, pH 6.8, 50% glycerol, 10% SDS, and 0.0625% bromophenol blue, ± 25% β-mercaptoethanol) and 1 μL of 1 M Tris base. Analyses were carried out according to Laemmli (*14*) using a Bio-Rad Mini Protean II electrophoresis system. Gels were stained for 30 min in Coomassie Blue staining solution (0.1% Coomassie Blue R-250 in 40% MeOH and 10% AcOH) and then destained for 12−15 h with 7.5% AcOH and 5% MeOH. Destained gels were scanned (ScanMaker 9600XL, Microtek) using Adobe Photoshop. As appropriate, band density was quantified using the National Institutes of Health Image program (version 1.61). Suitable controls demonstrated that band intensity was proportional to protein amount.

Enzyme Assay. All assays were performed at either room temperature (20−23 °C) or 37 °C in SB in a total volume of 80 μL, using S-2586 as substrate and monitoring the increase in A_{410} (*5*). In assays conducted in the presence of added salt, enzyme was preincubated with salt for 30 min prior to enzyme assay.

*Curve Fitting. Kinetics of PSA*ACT* Formation.* Values of k_{obs} were obtained by fits to eq 1, where $[E]_o$ is the total concentration of PSA added to the solution. The PSA*ACT* band was quantified as described above.

$$[\text{PSA*ACT*}] = [\text{E}]_o(1 - e^{-k_{obs}t}) \quad (1)$$

Values of k', the rate constant for PSA*ACT* formation at saturating [I], and K_I, the apparent dissociation constant for ACT binding to PSA, were determined by fitting k_{obs} values to eq 2.

$$k_{obs} = k' \times [\text{I}]_0/([\text{I}]_0 + K_I) \quad (2)$$

Fits to eqs 1 and 2 were carried out with Igor Pro 3.16 (Wavemetrics, Oswego, Oregon).

Scheme 1

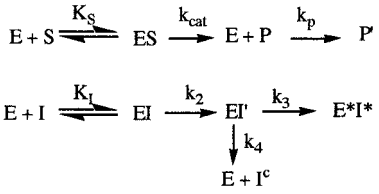

Scheme 2

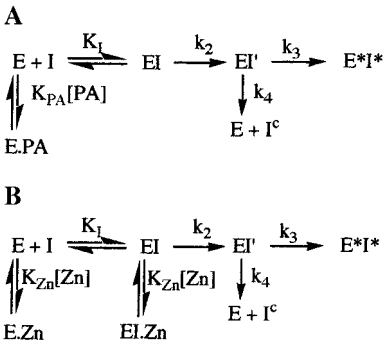

Kinetics of Inhibition of PSA by ACT. rPSA was added to an SB solution containing various concentrations of ACT and 0.5 mM S-2586, and the increase in A_{410} was monitored continuously. This increase is mainly due to *p*-nitroaniline (P) formation resulting from substrate hydrolysis. In addition, there is a slow decomposition of *p*-nitroaniline, yielding product(s), denoted P′, having higher ϵ_{410} than *p*-nitroaniline. From Scheme 1 (*15*), the change in A_{410} is given by eq 3, in which $\epsilon_{410,p}$ is the extinction coefficient of *p*-nitroaniline, and C is a constant term that is a function of k_p and $\epsilon_{410,p'}$, the apparent extinction coefficient of P′.

$$d(A_{410}/\epsilon_{410,p})/dt = k_{cat}[\text{ES}] + \text{C}[\text{P}] \quad (3)$$

A_{410} progress curves were fit to eq 3 and Scheme 1 by numerical integration (Micromath Scientist) yielding values for k_3 and C as fitted parameters. Fits were carried out using measured values of k_{cat}, K_S (as the Michaelis constant for S-2586), K_I, SI $[(k_3 + k_4)/k_3]$, and k' $[k_2k_3/(k_2 + k_3 + k_4)]$ (*16*). Evaluating k_3 permits evaluation of k_4, knowing SI, and of k_2, knowing k'.

For complex formation in the presence of polyamines or Zn^{2+}, rPSA was preincubated with inhibitors, rACT was added, and, following further incubation, the reaction mixture was quenched and analyzed by SDS−PAGE. The dependence of E*I* formation on [polyamine] or $[Zn^{2+}]$ was fit to Scheme 2, panels A or B, respectively, using determined values of K_I, k_2, k_3, and k_4, and yielding values for K_{PA} and K_{Zn}.

Proteolysis of PSA. PSA (1.8−3.6 μM) was incubated with subtilisin (Carlsberg and BPN′), type XVII−B protease from *Staphylococcus aureus* (stain V8), proteinase K, or trypsin. Protease concentration was 0.09−0.18 μM, except for trypsin (0.04 μM). Incubations were performed at 37 °C in SB for 0.5−1 h. Samples were analyzed by SDS−PAGE (20% gel) under reducing conditions.

Spectral Analysis. Fluorescence emission spectra employed excitation at 290 nm on a luminescence spectrometer (Hewlett-Packard). CD spectra (200−260 nm) were recorded

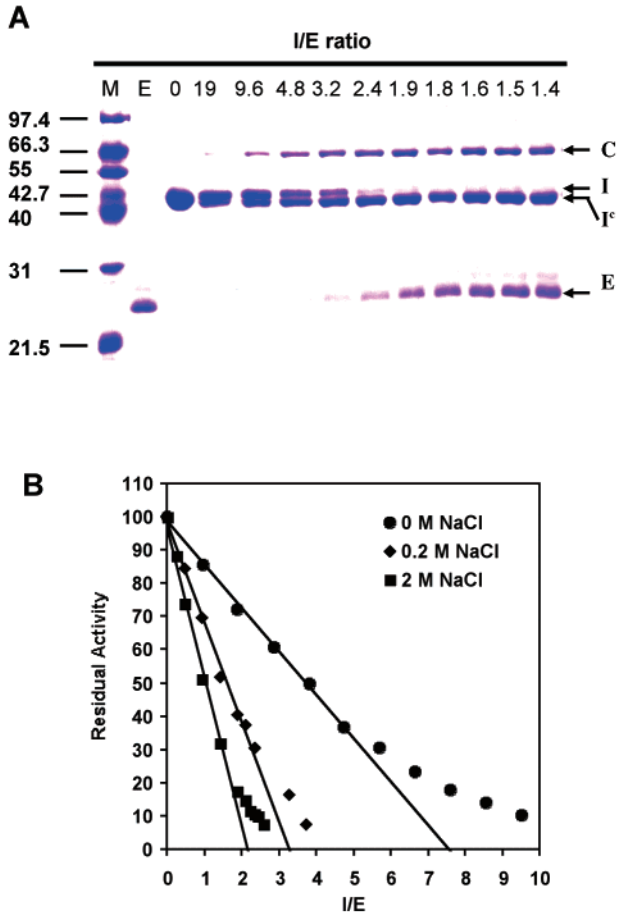

FIGURE 1: Stoichiometry of inhibition. (A) By nonreducing SDS−PAGE (12%) analysis. ACT (11.2 μM, 2.5 μL) was incubated with various added volumes of 2.9 μM PSA in 2.0 M NaCl and protein was precipitated with TCA. Lane 1, midrange protein markers; lane 2, PSA (5 μL); lanes 3−13, ACT/PSA as indicated. Arrows: C, PSA*ACT* complex; I, intact ACT; I^c, cleaved ACT; E, PSA. (B) By activity measure. Varying amounts of ACT were incubated with 1 μM PSA in the presence of 0 (●), 0.2 (♦), 2 (■) M NaCl. Following incubation, an equal volume of 1 mM S-2586 in SB was added and residual activity was determined at room temperature. Linear regression analysis of the decrease in protease activity with increasing [ACT] yielded estimates for SI. In both parts A and B, PSA and ACT were incubated in SB for 2 h at 37 °C prior to analysis.

on a CD spectrometer, model 62DS (AVIV, Lakewood, NJ). Spectra were taken on 2 μM PSA in SB at room temperature.

RESULTS

Stoichiometry of Inhibition (SI) of PSA by ACT. Reaction of PSA with rACT (Scheme 1) yields two products, one corresponding to the PSA*ACT* complex (the inhibitor pathway) and one giving rise to cleaved ACT (denote I^c) (the substrate pathway). Such branching is seen in a number of serpin−serine proteinase reactions (*15*, *17*), and is characterized by an SI (stoichiometry of inhibition) value, which is equal to the ratio of $(k_3 + k_4)/k_3$. The SI value at 2.0 M NaCl was determined to be 2.2 by SDS−PAGE analysis of the reaction of rACT with excess PSA (Figure 1A). This value was obtained from the intensity of the band corresponding to cleaved rACT following full reaction of rACT with excess PSA (lanes 9−13), as compared with the intensity of the band corresponding to the intact rACT added

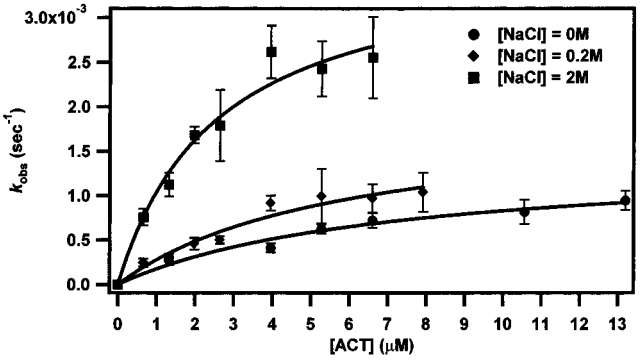

FIGURE 2: Rates of PSA*ACT* formation. rPSA (0.13 μM) and various amounts of excess ACT were incubated in SB at 37 °C ACT in the presence of 0 (●), 0.2 (♦), 2 (■) M NaCl. Aliquots were withdrawn at various times, quenched by addition of an equal volume of 20% TCA and subject to 12% SDS−PAGE analysis under reducing conditions. Fits of PSA*ACT* complex formation as a function of time at a given [ACT] to eq 1 yielded k_{obs} values. Plotted are k_{obs} values as a function of [ACT], fit to eq 2.

to the reaction mixture (lane 3). Values of SI at 0.0 and 0.2 M NaCl were higher, 7.5 and 3.2, respectively, as determined by comparison of titration curves of ACT inhibition of PSA activity at these NaCl concentrations with the curve at 2.0 M NaCl (Figure 1B). SI values of ∼2 have previously been reported for both cloned (*18*) and seminal plasma (*6*) PSA, and similar decreases in SI with rising [NaCl] are seen for human mast cell chymase interaction with ACT (*19*) and other serpins (*19*, *20*).

*Rate of PSA*ACT* Formation.* Apparent first-order rate constants for PSA*ACT* complex formation (k_{obs}) (eq 1) at fixed, excess ACT were determined in both the presence and absence of NaCl. The amounts of PSA*ACT* complex were determined by SDS−PAGE analysis of quenched reaction mixtures, as described previously (*10*, *21*). With the quench procedure employed, all forms of PSA not present as PSA*ACT* are seen as free PSA. Fitting of plots of the apparent first-order rate constants k_{obs} as a function of [ACT] to eq 2 (Figure 2) allowed determination of the values of K_I and k' displayed in Table 1. As these values make clear, the dependencies of K_I and k' on [NaCl] parallel those seen earlier (*5*) for K_m and k_{cat}, respectively. Thus, with added NaCl, K_I and K_m both decrease whereas k' and k_{cat} both increase. The magnitude of these changes are also similar. Relative to 0 NaCl, k_{cat}/K_m increases by 1.7- and 12-fold at 0.2 M NaCl and 2.0 M NaCl, respectively, whereas the corresponding factors for k'/K_I are 1.8- and 8-fold. The values of k'/K_I at 0 and 0.2 M NaCl are 2−4 times higher than a value reported earlier, measured at 37 °C in phosphate-buffered saline, in a more limited study using PSA purified from seminal fluid (*22*).

Slow Inhibition of PSA by ACT (Progress Curve). Addition of rPSA to solutions containing S-2586 and variable amounts of ACT led to slow inhibition kinetics, in which the amount of substrate hydrolyzed at infinite time drastically decreases as [ACT] is increased (Figure 3). The results obtained at 0, 0.2, and 2.0 M NaCl, were fit to eq 3 and Scheme 1, permitting evaluation of k_2, k_3, and k_4. Attempts to fit these results to a simpler scheme omitting EI′ were unsuccessful, even when the requirement that EI be in equilibrium with E and I was dropped. As is clear from the values presented in Table 1, the increase in k' with rising [NaCl] is due both to

Table 1: Rate and Equilibrium Constants[a]

[NaCl] (M)	K_S[b] (mM)	k_{cat}[b] (s^{-1})	k_{cat}/K_s[b] (M^{-1} s^{-1})	k_{cat}[c] (s^{-1})	SI	K_I (μM)	$10^3 k$ (s^{-1})	k'/K_I (M^{-1} s^{-1})	$10^3 k_2$ (s^{-1})	$10^3 k_3$ (s^{-1})	$10^3 k_4$ (s^{-1})
0	4.9 ± 0.3	0.25 ± 0.01	51 ± 3	0.87 ± 0.05	7.5 ± 0.1	7.8 ± 3.1	1.4 ± 0.2	180	13.9	5.7 ± 0.6	37
0.2	4.5 ± 0.4	0.40 ± 0.02	89 ± 9	1.2 ± 0.1	3.2 ± 0.1	5.8 ± 2.1	1.9 ± 0.4	330	8.7	6.2 ± 1.8	14
2	0.9 ± 0.1	0.53 ± 0.03	590 ± 60	4.1 ± 0.5	2.2 ± 0.1	2.6 ± 0.7	3.7 ± 0.4	1400	13.4	9.4 ± 2.0	11

[a] Determined at 37 °C except as otherwise noted. [b] Determined at 20−23 °C (*5*). [c] Derived from data in Figure 3, using K_S values determined earlier (*5*).

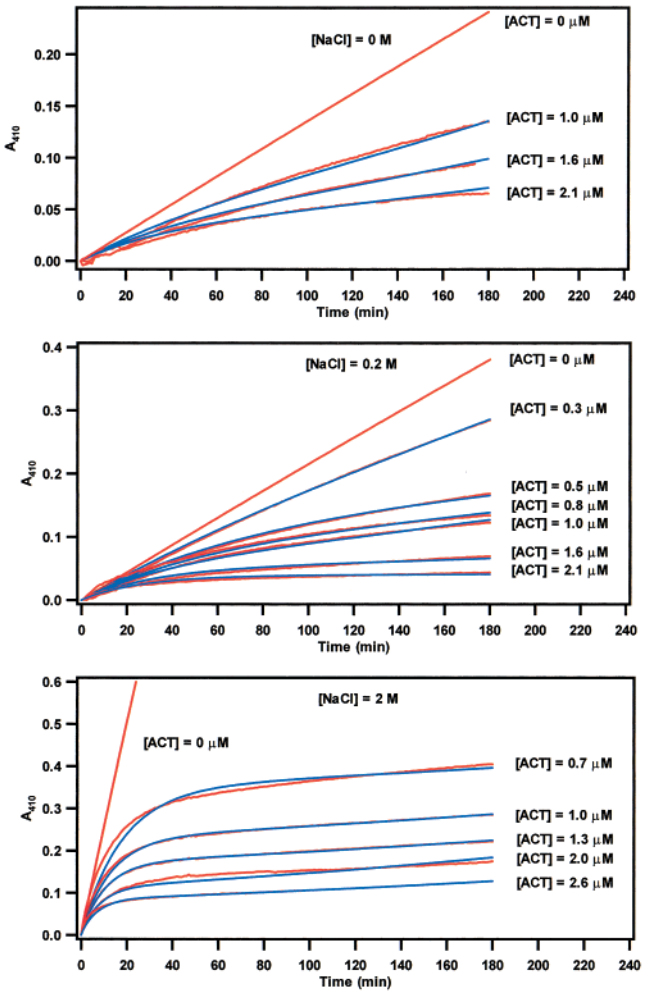

FIGURE 3: Slow inhibition of PSA by ACT. At zero time, PSA (33 nM) was added to an SB solution containing 0.5 mM S-2586 and various concentrations of ACT as indicated, at 37 °C, in the absence or presence of NaCl, and A_{410} was monitored continuously. Data were fit to Scheme 1, yielding estimates for k_2, k_3, and k_4 (Table 1). Experimental data, red lines; fits, blue lines.

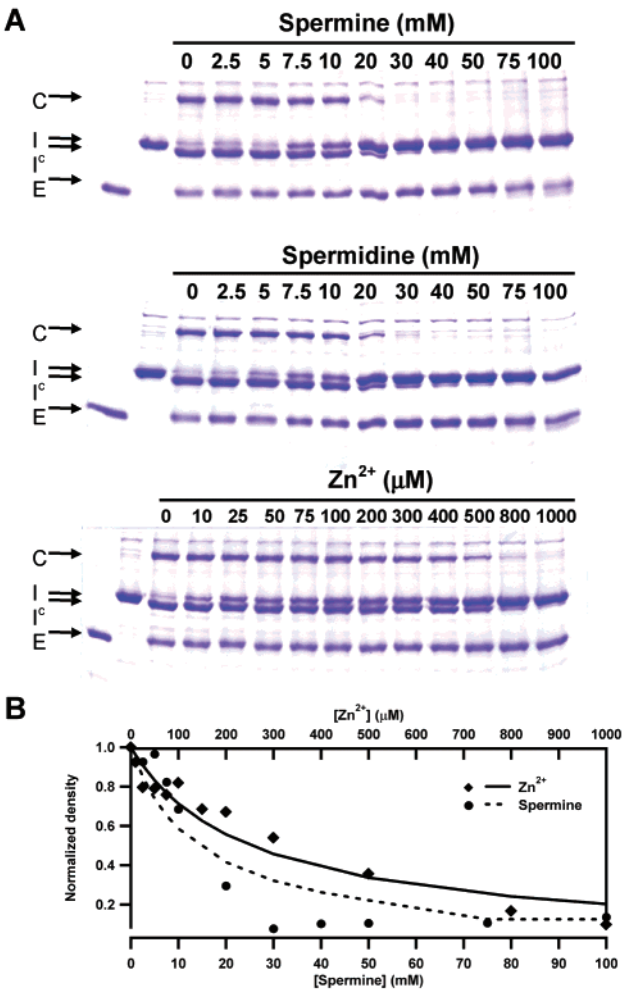

FIGURE 4: Polyamine and Zn^{2+} inhibition of PSA*ACT* formation. PSA (66 nM) preincubated in SB containing 2 M NaCl with various concentrations of inhibitors for 20 min at room temperature was further incubated with 150 nM ACT (all final concentrations) at 37 °C for 2 h. Reaction was stopped by TCA addition. (A) PSA*ACT* formation was analyzed by 12% SDS−PAGE under nonreducing conditions. The first two lanes are PSA and ACT controls. Arrows indicating PSA (E), ACT (I), cleaved ACT (I^c), and PSA*ACT* complex (C) are shown. (B) Normalized density of the complex band was fit to Scheme 2, panel A [(●), spermine] or panel B [(♦), Zn^{2+}].

increased k_3 and decreased k_4. In contrast, the value of k_2 shows no clear trend as a function of [NaCl].

*Inhibitory Effect of Polyamines and Zn^{2+} on PSA*ACT* Formation.* Both the polyamines spermine and spermidine, and Zn^{2+}, are present in high concentrations in seminal plasma and are inhibitors of PSA proteolytic activity. Spermine and Zn^{2+} are competitive and noncompetitive inhibitors, respectively (*5*). As shown in Figure 4A, all three inhibitors also inhibit PSA*ACT* complex formation. Fitting the dependence of PSA*ACT* formation on [spermine] or [Zn^{2+}] to Scheme 2, panels A or B, respectively (Figure 4B), yields values of K_{PA} (spermine, 5 ± 4 mM) and K_{Zn} (75 ± 4 μM) that are comparable to those obtained earlier (*5*) from inhibition of PSA proteolytic activity, measured at 20−23 °C (2 mM and 50−78 μM, respectively).

Conformation Change Induced by NaCl. The acceleration caused by added NaCl of both PSA reaction with ACT and PSA turnover of S-2586 (Table 1) implies that NaCl induces conformational change in PSA, since no such acceleration is seen, for example, for Chtr reaction either with standard substrates or with ACT (*8*). Direct evidence for such conformational change is provided by examination of the

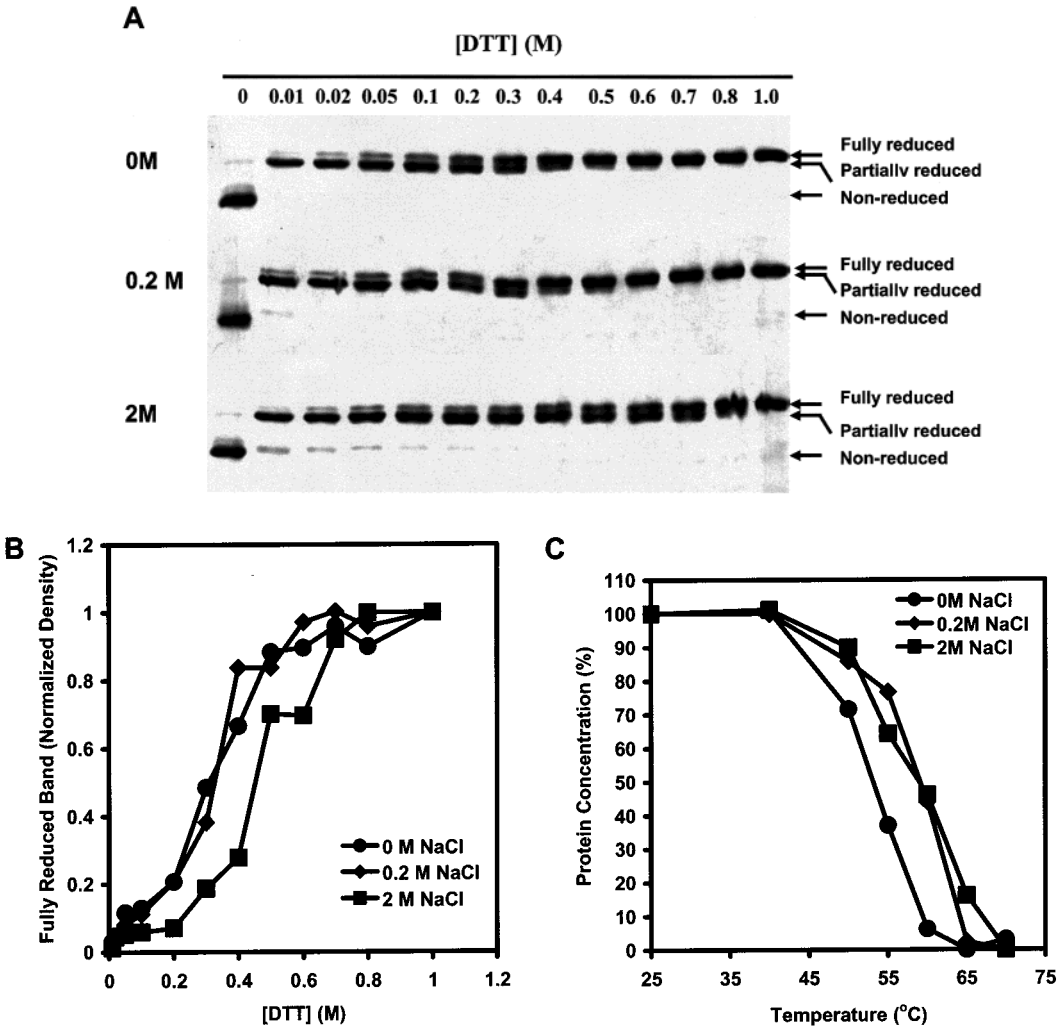

FIGURE 5: NaCl effects on PSA Conformation. Experiments were conducted in the presence of 0 (●), 0.2 M (♦), or 2 M NaCl (■) in SB. (A) DTT reduction. PSA (0.6 μg in 20 μL) was incubated with various concentrations of DTT, as indicated, for 1 h at room temperature. Iodoacetamide was added at a concentration equal to that of DTT and the mixture was allowed to stand for another 20 min at room temperature. Protein was precipitated by TCA addition. Samples were analyzed by SDS−PAGE (12% gel) under nonreducing conditions. Arrows indicate bands corresponding to nonreduced, partially reduced, and fully reduced forms of PSA. (B) Plots of band density of fully reduced form of PSA as a function of [DTT]. (C) Heat-induced precipitation. PSA (0.14 mg/mL) was incubated at various temperatures for 10 min, followed by centrifugation (16000*g*, 10 min). At each temperature, protein remaining in the supernatant was determined by Bradford analysis.

dependencies on added NaCl of both DTT reduction and thermal denaturation of PSA (Figure 5).

PSA reduction by DTT proceeds via at least one intermediate, as shown by SDS−PAGE analysis (Figure 5, panels A and B). While partial reduction is achieved at quite low [DTT] in both the absence and presence of added NaCl, as NaCl concentration is increased full reduction requires higher [DTT]. Similarly, thermal denaturation of PSA, as measured by heat-induced precipitation, requires higher temperatures in the presence of NaCl than in its absence (Figure 5C).

These changes cannot be rationalized with a simple two-state model, since they have different dependencies on [NaCl]. Thus, whereas addition of 0.2 M NaCl hardly changes the concentration of DTT required for full reduction and a marked increase is only seen in the presence of 2 M NaCl, addition of 0.2 M NaCl is sufficient to increase the temperature for 50% PSA precipitation from 52 to 58 °C, and little additional increase results from further raising NaCl to 2.0 M. The comparative effects of added NaCl on K_m and k_{cat} for S-2586 hydrolysis (*5*, Table 1) also lead to the conclusion that added NaCl induces more than one conformational change.

Such conformational changes may be quite limited in scope. Thus, neither intrinsic fluorescence, circular dichroism (200−260 nm), nor the partial digestion patterns produced by various proteases acting on PSA (subtilisin, type XVII-B protease, proteinase K, or trypsin) were appreciably affected by addition of NaCl up to 2.0 M (data not shown). However, in work published after the original submission of this paper, Huang et al. (*23*) report significant alteration in the near-UV CD spectrum of PSA (260−300 nm) on addition of 0.5 M Na_2SO_4.

*Proteolysis of PSA*ACT**. As is true for other Chtr*ACT* (*8*), PSA*ACT* is subject to proteolytic degradation by HNE (Figure 6A, lanes 5−18). A separate control experiment (lanes 1 and 2) demonstrates that PSA alone is stable toward HNE hydrolysis under similar conditions. Loss of the electrophoretic band corresponding to PSA*ACT* is accompanied by formation of two transient bands X_1 and X_2, having apparent molecular masses slightly larger and con-

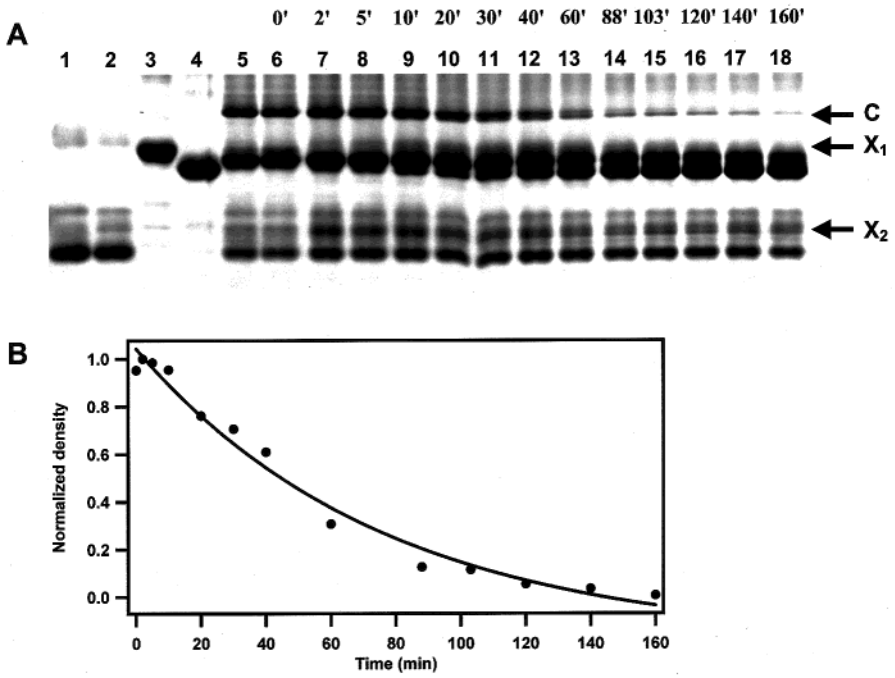

FIGURE 6: PSA*ACT* complex degradation by HNE. (A) PSA (3.4 μM) was preincubated for 5 h with ACT (5.6 μM) in SB containing 0.2 M NaCl. HNE (final concentration, 0.6 μM) was then added for various periods of time. Reactions were quenched by addition of TCA. All steps were carried out at 37 °C. Quenched samples were analyzed by SDS−PAGE under nonreducing conditions. Lane 1, PSA control; lane 2, PSA treated with HNE for 3 h; lane 3, ACT control; lane 4, ACT treated with HNE for 3 h; lane 5, PSA incubated with ACT for 8 h without HNE treatment. Arrows: C indicates PSA*ACT* complex, X_1 and X_2 are proteolysis products. Lanes 6−18, PSA/ACT complex treated with HNE for the times indicated. (B) Density of band C as a function of time of HNE digestion. The line is a first-order decay fit.

siderably smaller than that of intact ACT, respectively. As neither of these bands is seen on HNE proteolysis of ACT alone, they must represent products of PSA*ACT* proteolysis which are themselves unstable toward further proteolysis. The apparent rate constant for loss of PSA*ACT*, 2.3×10^{-4} s^{-1}, corresponds to a calculated second-order rate of 400 M^{-1} s^{-1} at 37 °C (pH 7.8), which is considerably slower than the value of 30 000 M^{-1} s^{-1} at 25 °C (pH 7) previously found for HNE proteolysis of Chtr*ACT* (*17*). Thus, the target of HNE proteolysis is less exposed in PSA*ACT* than in Chtr*ACT*. By analogy with Chtr*ACT* (*8*) and other E*I* complexes (*24*−*26*), we presume this target to be the PSA moiety in PSA*ACT*.

DISCUSSION

PSA Interaction with ACT. Our results provide strong evidence for the presence of at least one intermediate, EI′, between the EI encounter complex and the E*I* acyl−enzyme complex formed on reaction of PSA and ACT. This conclusion is based on our ability to satisfactorily fit two independent measures of PSA interaction with ACT to Scheme 1, as presented in Figures 2 (PSA*ACT* formation) and 3 (inhibition of PSA), which contrasts with our inability to obtain satisfactory fits to a simpler scheme omitting EI′. In Scheme 1, which conforms to the classic scheme for serpin:proteinase interactions having an SI > 1 (*15*, *17*), equilibration of E and I with EI is followed by two first-order processes, characterized by rate constants k_2 and k_3, leading to E*I* formation, with a branching step, leading to cleaved I (I^c) formation, characterized by rate constant k_4.

PSA has been considered as a Chtr-like enzyme, and it is noteworthy that the PSA*ACT* complex is similar to the Chtr*ACT* complex in two important respects. First, the k_2/k_3 ratio of 1.4−2.4 for all three salt conditions (Table 1) parallels the value of 1.5−2.0 obtained when rate data for Chtr*ACT* formation, obtained under similar conditions (pH 7, 40 °C), were fit to Scheme 1 (*21*). Second, it is subject to proteolysis by HNE (Figure 5), as is the Chtr*ACT* complex (*8*). Indeed, protease digestion of E*I* complexes may be a general phenomenon (*8*, *24*−*26*).

However, we find two significant differences as well, each making ACT a less efficient inhibitor of PSA than of Chtr. In particular, PSA has a much higher SI value for interaction with ACT (7.5−2.2, Table 1) vs a value of 1.0 for Chtr (*11*, *17*). Also, PSA reacts much more slowly with ACT, with values for k_2 and k_3 (Table 1) some 3−4 orders of magnitude lower than those found for Chtr (*21*). Also contributing to the poor reactivity of PSA with ACT is the relatively high value for K_I, 3−8 μM. By contrast, the value for cathepsin G interaction with ACT is 0.06 μM (*27*) and other cognate serine proteinase:serpin complexes have values ranging from 0.09 to 0.5 μM (*28*−*30*). These differences lead to apparent second-order rate constants for ACT inhibition of PSA (200−1400 M^{-1} s^{-1}), even when multiplied by SI to correct for the substrate pathway (giving a range of 1500−3100 M^{-1} s^{-1}), that are much lower than those observed for reaction of ACT with either Chtr or cathepsin G, for which the corresponding constants are 1×10^6 M^{-1} s^{-1} (*11*) and 5×10^7 M^{-1} s^{-1} (*31*), respectively. Such low rate constants for serpin-serine proteinase pairs are, however, not without precedent. Thus, Factor XIa reacts with C1 inhibitor, α_1-proteinase inhibitor, α_2-antiplasmin, and antithrombin III with rate constants of 1.8, 0.1, 0.43, and 0.32×10^3 M^{-1} s^{-1}, respectively (*32*), and the direct reaction of thrombin with antithrombin III has a rate constant of 2.5×10^3 M^{-1} s^{-1} (*33*).

The low reactivity of PSA toward ACT parallels its low reactivity toward the standard substrate S-2586, for which the k_{cat} and k_{cat}/K_m values found previously are also 10^3-10^4 less than those found for Chtr (*34*). This parallelism is also seen with respect to the activating effects of NaCl and the inhibitory effects of polyamines and Zn^{2+} (see Results) and is not unexpected, since both E*I* formation and substrate turnover involve acyl-enzyme formation. Such low reactivity may be a direct result of two features of PSA structure.

Although no crystal structure of PSA itself has been reported, high-resolution structures are available for other kallikreins and for the related proteinase tonin, including some complexed with small protein inhibitors (*35*−*41*), and have been used to construct structural models for PSA (*42*−*44*) and the PSA·ACT complex (*45*). As noted by Bode et al. (*35*), loops surrounding the active site form a circular wall that is much more prominent in porcine pancreatic kallikrein than, for instance, in trypsin, and might contribute to the restricted accessibility of the kallikrein active site vs the trypsin active site. In addition, vis-à-vis proteinases such as Chtr and trypsin, kallikreins contain a characteristic loop inserted at position 95 (Chtr numbering) that is both highly flexible and proximal to the active site (*40*). Both of these features are preserved in models of PSA structure. Furthermore, molecular dynamics simulations suggest that the kallikrein loop can exist in two conformations, a "closed" form in which access to the active site is restricted, and an "open" form with an accessible active site (*42*), although only the open form has been seen experimentally (*40*).

In light of these results, it is tempting to speculate that the apparent structural changes induced in PSA by added NaCl correspond to a change from the closed to the open conformation, although, as we have seen, more than two states must be involved. Given the observed reduction in SI, such a change would favor not only a catalytically more active form of PSA, but also the inhibitory pathway over the substrate pathway (step 3 vs step 4 in Scheme 1) in the PSA·ACT complex.

Potential Clinical Implications of This Work. PSA is of clinical interest both because of its utility as a serum marker in the diagnosis of prostate cancer and of its possible role as an agent in the development of prostate and other cancers. Due to the relatively high levels of ACT in the serum [2−10 μM, with the higher levels reached in acute phase (*46*)], the bulk of PSA found in the serum is in the form of the PSA*ACT* complex. Sophisticated immunochemical assays have been developed to determine serum levels of both complexed PSA and free PSA and to relate such levels to disease states (*3*). Our results demonstrating HNE proteolysis of the PSA*ACT* complex (Figure 6) have potential consequences for such assays, since enzymatically active HNE levels as high as ∼40 nM in blood serum have been reported (*47*). It would thus clearly be of interest to examine the effect of HNE on the efficiency of antibody recognition of the complex, and if significant effects are found, to locate the major sites of cleavage within the HNE-proteolyzed complex.

The role of PSA catalytic activity in cancer development is poorly understood and likely to be complex. As recently reviewed (*4*), while PSA proteolysis of insulin-like growth factor binding protein-3, the latent form of transforming growth factor-β, and basement membrane proteins have been linked to proliferation of prostatic stromal and epithelial cells (*48*−*50*), tumor spread (*51*), and invasion and metastasis (*52*), PSA has also been shown to be a tumor suppressor (*53*), a negative regulator of cell growth (*54*), and an angiogenesis inhibitor (*55*, *56*). These results suggest that both up- and downregulation of PSA activity in vivo could have important therapeutic applications. Understanding the regulation of PSA activity in vivo is also important for optimizing attempts to use PSA-specific pro-drugs for treatment of advanced prostate cancer (*57*, *58*).

Our results provide important information toward such an understanding. It is generally agreed that active PSA released into human serum reacts principally with two inhibitors, α_2-macroglobulin and ACT. Reaction with α_2-macroglobulin is favored by a factor of approximately two (*6*, *22*, *59*). That the PSA−ACT complex is nonetheless the predominant form of PSA found in serum is due to faster clearance of the PSA−α_2-macroglobulin complex than of the PSA-ACT complex (*60*, *61*). However, in interstitial fluid surrounding PSA-producing cells, where [ACT] ≫ [α_2-macroglobulin], the PSA-ACT complex is likely to be dominant (*6*). Our results, in determining rate and equilibrium constants involved in PSA*ACT* formation, demonstrate that it will take considerable time for all of the catalytically active PSA released into such fluid to be converted to the inactive PSA*ACT* complex, even if the level of ACT present in such fluid were to attain that present in serum. For example, in 0.2 M NaCl at ∼8 μM ACT, 15−20% of PSA remains active after 10 min (Table 1), and this percentage would be further increased in the presence of substrate (Scheme 1). Thus, when PSA is being continuously released into interstitial fluid, active PSA can build to appreciable steady-state levels, making possible hydrolysis of protein substrates by PSA, even in the presence of large excesses of ACT. A similar argument can be made for buildup of steady-state levels in serum, but the values would necessarily be lower because of PSA complexation by α_2-macroglobulin.

While efforts to inhibit PSA activity have relied on a classical active-site directed approach (*43*), our evidence that PSA exists in several conformations with differing reactivity toward both substrates and ACT raises the prospect that other agents, either endogeneous or exogenous, can be found that would raise PSA activity levels by mimicking the effects of NaCl [or of Na_2SO_4 (*23*) or glycerol (*5*)]. A 13-mer peptide, selected from a random library, that binds to PSA and increases its specific activity may provide an example of just such an agent (*62*). Although higher PSA specific activity would not necessarily result in an increase in total PSA activity in interstitial fluid or serum, where it could be offset by an increased rate of PSA reaction with ACT and possibly α_2-macroglobulin, such an increase should occur in tissues containing levels of PSA exceeding those of these inhibitors, such as prostate (*1*, *63*) and possibly breast (*4*) tissue.

ACKNOWLEDGMENT

We thank Ms. Nora Zuño for excellent technical assistance.

REFERENCES

1. Lilja, H. (1997) *Br. J. Urol. 79* (Suppl. 1), 44−48.

2. Stamey, T. A., Yang, N., Hay, A. R., McNeal, J. E., Freiha, F. S., and Redwin, E. A. (1987) *N. Engl. J. Med. 317*, 909−916.
3. Catalona, W. J., Partin, A. W., Slawin, K. M., Brawer, M. K., Flanigan, R. C., Patel, A., Richie, J. P., deKernion, J. B., Walsh, P. C., Scardino, P. T., Lange, P. H., Subong, E. P., Parson, R. E., Gasior, G. H., Loveland, K. G., and Southwick, P. C. (1998) *J. Am. Med. Assoc. 279*, 1542−1547.
4. Diamandis, E. P. (2000) *Clin. Chem. 46*, 896−900.
5. Hsieh, M.-C., and Cooperman, B. S. (2000) *Biochim. Biophys. Acta 1481*, 75−87.
6. Christensson, A., Laurell, C. B., and Lilja, H. (1990) *Eur. J. Biochem. 194*, 755−763.
7. Malm, J., Hellman, J., Hogg, P., and Lilja, H. (2000) *Prostate 45*, 132−139.
8. Stavridi, E., O'Malley, K., Lukacs, C., Moore, W. T., Lambris, J. D., Christianson, D., Rubin, H., and Cooperman, B. S. (1996) *Biochemistry 35*, 10608−10615.
9. Wilczynka, M., Fa, M., Ohlsson, P. I., and Ny, T. (1995) *J. Biol. Chem. 270*, 29652−29655.
10. Nair, S. A., and Cooperman, B. S. (1998) *J. Biol. Chem. 273*, 17459−17462.
11. Rubin, H., Wang, Z. M., Nickbarg, E. B., McLarney, S., Naidoo, N., Schoenberger, O., Johnson, J., and Cooperman, B. S. (1990) *J. Biol. Chem. 265*, 1199−1207.
12. Bradford, M. M. (1976) *Anal. Biochem. 72*, 248−254.
13. Luo, Y., Zhou, Y., and Cooperman, B. S. (1999) *J. Biol. Chem. 274*, 17733−17741.
14. Laemmli, U. K. (1970) *Nature 227*, 680−685.
15. Gettins, P. G. W., Patson, P. A., and Olson, S. T. (1996) *Serpins: Structure, Function, and Biology*, Chapter 3, R. G. Landes, Austin, TX.
16. Fersht, A. (1999) *Structure and Mechanism in Protein Science*, p 124, W. H. Freeman, New York.
17. Cooperman, B. S., Stavridi, E., Nickbarg, E., Rescorla, E., Schechter, N. M., and Rubin, H. (1993) *J. Biol. Chem. 268*, 23616−23625.
18. Takayama, T. K., Fujikawa, K., and Davie, E. W. (1997) *J. Biol. Chem. 272*, 21582−21588.
19. Schechter, N. M., Sprows, J. L., Schoenberger, O. L., Lazarus, G. S., Cooperman, B. S., and Rubin, H. (1989) *J. Biol. Chem. 264*, 21308−21315.
20. Schick, C. Kamachi, Y., Bartuski, A. J., Cataltepe, S., Schechter N. M., Pemberton, P. A., and Silverman, G. A. (1997) *J. Biol. Chem. 272*, 1849−1855.
21. O′Malley, K. M., Nair, S. A., Rubin, H., and Cooperman, B. S. (1997) *J. Biol. Chem. 272*, 5354−5359.
22. Otto, A., Bar, J., and Birkenmeier, G. (1998) *J. Urol. 159*, 297−303.
23. Huang, X., Knoell, C. T., Frey, G., Hazegh-Azam, M., Tashjian, A. H., Jr., Hedstrom, L., and Abeles, R. H. (2001) *Biochemistry 40*, 11734−11741.
24. Kaslik, G., Kardos, J., Szabo, E., Szilagyi, L., Zavodszky, P., Westler, W. M., Markley, J. L., and Graf, L. (1997) *Biochemistry 36*, 5455−5464.
25. Huntington, J. A., Read, R. J., and Carrell, R. W. (2000) *Nature 407*, 923−926.
26. Egelund, R., Petersen, T. E., and Andreasen, P. A. (2001) *Eur. J. Biochem. 268*, 673−685.
27. Duranton, J., Adam, C., and Bieth, J. G. (1998) *Biochemistry 37*, 11239−11245.
28. Mellet, P., Boudier, C., Mely, Y., and Bieth, J. G. (1998) *J. Biol. Chem. 273*, 9119−9123.
29. Kvassman, J. O., Verhamme, I., and Shore, J. D. (1998) *Biochemistry 37*, 15491−15502.
30. Lawrence, D. A., Olson, S. T., Muhammad, S., Day, D. E., Kvassman, J.-O., Ginsburg, D., and Shore, J. D. (2000) *J. Biol. Chem. 275*, 5839−5844.
31. Beatty, K., Bieth, J., and Travis, J. (1980) *J. Biol. Chem. 255*, 3931−3934.
32. Wuillemin, W. A., Eldering, E., Citarella, F., de Ruig, C. P., ten Cate, H., and Hack, C. E. (1996) *J. Biol. Chem. 271*, 12913−12918.
33. Holmes, W. E., Lijnene, H. R., and Collen, D. (1987) *Biochemistry 26*, 5133−5140.
34. Tozser, J., Szabo, G., Pozsgay, M., Aurell, L., and Elodi, P. (1986) *Acta Biochim. Biophys. Hung. 21*, 335−348.
35. Bode, W., Chen, Z., Bartels, K., Kutzbach, C., Schmidt-Kastner, G., and Bartunik, H. (1983) *J. Mol. Biol. 164*, 237−282.
36. Bode, W., and Chen, Z. (1983) *J. Mol. Biol. 164*, 283−311.
37. Fujinaga, M., and James, M. N. G. (1987) *J. Mol. Biol. 195*, 373−396.
38. Bax, B., Blundell, T. L., Murray-Rust, J., and McDonald, N. Q. (1997) *Structure 5*, 1275−1285.
39. Mittl, P. R., Di Marco, S., Fendrich, G., Pohlig, G., Heim, J., Sommerhoff, C., Fritz, H., Priestle, J. P., and Grutter, M. G. (1997) *Structure 5*, 253−264.
40. Timm, D. E. (1997) *Protein Sci. 6*, 1418−1425.
41. Katz, B. A., Liu, B., Barnes, M., and Springman, E. B. (1998) *Protein Sci. 7*, 875−885.
42. Villoutreix, B. O., Getzoff, E. D., and Griffin, J. H. (1994) *Protein Sci. 3*, 2033−2044.
43. Coombs, G. S., Bergstrom, R. C., Pellequer, J. L., Baker, S. I., Navre, M., Smith, M. M., Tainer, J. A., Madison, E. L., and Corey, D. R. (1998) *Chem. Biol. 5*, 475−488.
44. Adlington, R. M., Baldwin, J. E., Becker, G. W., Chen, B., Cheng, L., Cooper, S. L., Hermann, R. B., Howe, T. J., McCoull, W., McNulty, A. M., Neubauer, B. L., and Pritchard, G. J. (2001) *J. Med. Chem. 44*, 1491−1508.
45. Villoutreix, B. O., Lilja, H., Pettersson, K., Lovgren, T., and Teleman, O. (1996) *Protein Sci. 5*, 836−851.
46. Travis, J., and Salvesen, G. S. (1983) *Annu. Rev. Biochem. 52*, 655−709.
47. Hornebeck, W., Brechemier, D., Jacob, M. P., Frances, C., and Robert, L. (1984) *Adv. Exp. Med. Biol. 167*, 111−119.
48. Cohen, P., Peehl, D. M., Graves, H. C. B., and Rosenfeld, R. G. (1994) *J. Endocrinol. 142*, 407−415.
49. Pollak, M., Beamer, W., and Zhang, J. C. (1998) *Cancer Metastasis Rev. 17*, 383−390.
50. Sutkowski, D. M., Goode, R. L., Baniel, J,. Teater, C., Cohen, P., McNulty, A. M., Hsiung, H. M., Becker, G. W., and Neubauer, B. L. (1999) *J. Natl. Cancer Inst. 91*, 1663−1669.
51. Killian, C. S., Corral, D. A., Kawinski, E., and Constantine, R. I. (1993) *Biochem. Biophys. Res. Commun. 192*, 940−947.
52. Webber, M. M., Waghray, A., and Bello, D. (1995) *Clin. Cancer Res. 1*, 1089−1094.
53. Balbay, M. D., Juang, P., Ilansa, N., Williams, S., McConkey, D., Fidler, I. J., and Pettaway, C. A. (1999) *Proc. Am. Assoc. Cancer Res. 40*, 225−226.
54. Lai, L. C., Erbas, H., Lennard, T. W., and Peaston, R. T. (1996) *Int. J. Cancer 66*, 743−746.
55. Fortier, A. H., Nelson, B. J., Grella, D. K., and Holaday, J. W. (1999). *J. Natl. Cancer Inst. 91*, 1635−1640.
56. Heidtmann, H. H., Nettelbeck, D. M., Mingels, A., Jager, R., Welker, H. G., and Kontermann, R. E. (1999) *Br. J. Cancer 81*, 1269−1273.
57. Khan, S. R., and Denmeade, S. R. (2000) *Prostate 45*, 80−83.
58. DeFeo-Jones, D., Garsky, V. M., Wong, B. K., Feng, D. M., Bolyar, T., Haskell, K., Kiefer, D. M., Leander, K., McAvoy, E., Lumma, P., Wai, J., Senderak, E. T., Motzel, S. L., Keenan, K., Van Zwieten, M., Lin, J. H., Freidinger, R., Huff, J., Oliff, A., and Jones, R. E. (2000) *Nat. Med. 6*, 1248−1252.
59. Leinonen. J., Zhang, W. M., and Stenman, U. H. (1996) *J. Urol. 155*, 1099−1103.
60. Birkenmeier, G., Struck, F., and Gebhardt, R. (1999) *J. Urol. 162*, 897−901.
61. Zhang, W. M., Finne, P., Leinonen, J., and Stenman, U. H. (2000) *Scand J. Clin. Lab. Invest. Suppl. 233*, 51−58.
62. Wu, P., Leinonen, J., Koivunen, E., Lankinen. H., and Stenman, U. H. (2000) *Eur. J. Biochem. 267*, 6212−6220.
63. Ornstein, D. K., Englert, C., Gillespie, J. W., Paweletz, C. P., Linehan, W. M., Emmert- Buck, M. R., and Petricoin, E. F., III (2000) *Clin. Cancer Res. 6*, 353−356.

BI0117450